

2014

# Earth-Impact Modeling and Analysis of a Near-Earth Object Fragmented and Dispersed by Nuclear Subsurface Explosions<sup>1</sup>

Brian Kaplinger,<sup>2</sup> Bong Wie,<sup>3</sup> and David Dearborn<sup>4</sup>

## Abstract

Although various technologies, including nuclear explosions, kinetic impactors, and slow-pull gravity tractors, have been proposed for mitigating the impact threat of near-Earth objects (NEOs), there is no consensus on how to reliably deflect or disrupt such hazardous NEOs in a timely manner. This paper describes the orbital dispersion modeling, analysis, and simulation of an NEO fragmented and dispersed by nuclear subsurface explosions. It is shown that various fundamental approaches of Keplerian orbital dynamics can be effectively employed for the orbital dispersion analysis of fragmented NEOs. This paper also shows that, under certain conditions, proper disruption using a nuclear subsurface explosion with shallow burial is a feasible strategy, providing considerable impact damage reduction if all other approaches fail.

## Introduction

Despite the lack of a known immediate threat from a near-Earth object (NEO) impact, historical scientific evidence suggests that the potential for a major catastrophe created by an NEO impacting Earth is very real. It is a matter of when, and humankind must be prepared for it.

If an NEO on an Earth-impacting course can be detected with a mission lead-time of at least several years, the challenge becomes mitigating its threat. For

<sup>1</sup>This paper was published previously as AAS 10–137 at 20th AAS/AIAA Space Flight Mechanics Meeting, San Diego, CA, Feb. 15–17, 2010.

<sup>2</sup>Ph.D. Graduate Research Assistant, Asteroid Deflection Research Center, Department of Aerospace Engineering, Iowa State University, 2271 Howe Hall, Room 2325, Ames, IA 50011-2271. E-mail: bdkaplin@iastate.edu.

<sup>3</sup>Vance Coffman Endowed Chair Professor, Asteroid Deflection Research Center, Department of Aerospace Engineering, Iowa State University, 2271 Howe Hall, Room 2325, Ames, IA 50011-2271. E-mail: bongwie@iastate.edu.

<sup>4</sup>Research physicist/astrophysicist, Lawrence Livermore National Laboratory, 7000 East Avenue, Livermore, CA 94550. E-mail: dearborn2@llnl.gov.

a small body impacting in a sufficiently unpopulated region, mitigation may simply involve evacuation. However, larger bodies, or bodies impacting sufficiently developed regions may be subjected to mitigation by either disrupting (i.e., destroying or fragmenting with large dispersion), or by altering its trajectory so that it will miss Earth. When the time to impact exceeds a decade, the velocity perturbation needed to alter the orbit is small ( $\approx 2$  cm/s) [1]. A variety of schemes, including nuclear standoff explosions, kinetic impactors, and slow-pull gravity tractors, have already been extensively investigated for the NEO deflection problem [1–10]. The feasibility of each approach to deflect an incoming hazardous NEO depends on its size, spin rate, composition, the mission lead-time, and many other factors. When the time to impact is short, the necessary velocity change required for deflecting a target NEO may become impractically large and thus a fragmentation/dispersion may become the only viable option.

Because nuclear energy densities are nearly a million times higher than those possible with chemical bonds, it is the most mass-efficient means for storing energy with today's technology. Consequently, a nuclear standoff explosion, which is often considered as the preferred approach among the nuclear options, is much more effective than all other non-nuclear alternatives, especially for larger NEOs with a short mission lead time [1–4]. Another nuclear technique, involving the subsurface use of nuclear explosives, is in fact more efficient than the standoff explosion. The nuclear subsurface method, even with shallow burial ( $<5$  m), delivers large energy so that there is a likelihood of totally disrupting the NEO. A common concern for such a powerful nuclear option is the risk that fragmentation of the NEO could substantially increase the damage upon Earth impact of the resulting fragments, as discussed in references [1–3, 7], and [11–13]. In fact, if the NEO breaks into a small number of large fragments capable of surviving reentry, the multiple impacts on Earth might cause far more damage than a single, larger impact. Thus, the nuclear disruption approach has not been recommended as a valid technique for mitigation in a recent NEO study report by National Research Council's Committee to Review Near-Earth Object Surveys and Hazard Mitigation Strategies [7]. Additional research, including a suite of independent calculations and laboratory experiments, but particularly including experiments on real comets and asteroids, has been recommended to prove that nuclear disruption can be a valid method [7].

However, despite various uncertainties inherent to the nuclear disruption approach, disruption can become an effective strategy if most fragments disperse at speeds in excess of the escape velocity so that a very small fraction of fragments impact the Earth. This paper will show that, for some representative cases (principally when the warning time is very short), disruption is a feasible strategy, especially if all other deflection approaches were to fail.

A critical element of any mitigation strategy is the capability of available launch vehicles. A preliminary conceptual design of an interplanetary ballistic missile (IPBM) system carrying nuclear payloads is presented in reference [9]. The proposed IPBM system consists of a launch vehicle (LV) and an integrated space vehicle (ISV). The ISV consists of an orbital transfer vehicle and a terminal maneuvering vehicle carrying nuclear payloads. A Delta IV Heavy launch vehicle can be chosen as a baseline LV of a primary IPBM system for delivering a 1500-kg (mass) nuclear explosive for a rendezvous mission with a target NEO. A secondary IPBM system using a Delta II class launch vehicle (or a Taurus II), with a smaller ISV carrying a 500-kg nuclear explosive, is also described in reference [9]. For

most threatening NEO orbits, a primary IPBM system studied in reference [9] can deliver a 1.5-Mt nuclear payload while a secondary system can deliver a 500-kt nuclear payload. A kiloton (kt) of TNT is equal to  $4.18 \times 10^{12}$  J.

This paper presents the fundamentals of orbital dispersion modeling, analysis, and simulation of an NEO fragmented and dispersed by nuclear subsurface explosions. This paper demonstrates that various fundamental approaches of Keplerian orbital dynamics (e.g., references [14–16]) can be effectively employed for the orbital dispersion analysis of disrupted NEOs.

## Orbital Dispersion Modeling

### Basic Problem Formulation

All of the orbital analysis and simulation results presented in this paper have been validated using the various fundamental approaches of Keplerian orbital dynamics described in this section. The Standard Dynamical Model (SDM) of the Solar System for trajectory predictions of NEOs normally includes the gravity of the Sun, planets, Moon, and at least the three largest asteroids. However, significant orbit prediction error can result even using the SDM due to the unmodeled or mismodeled non-gravitational perturbation accelerations caused by the Yarkovsky effect and solar radiation pressure. The Yarkovsky effect is the thermal radiation thrust due to the anisotropic re-radiation of heat from a rotating body in space [17]. Consequently, in this paper we consider a fictive NEO on an Earth-impacting course along its nominal Keplerian trajectory and then examine the orbital dispersion of the NEO fragmented by a nuclear subsurface explosion. The effect of the mutual gravitational forces from all fragments (i.e., the self-gravity effect) is not considered in this paper because the fragments (caused by nuclear subsurface explosions) disperse at speeds much greater than the escape velocity. However, a preliminary study result for the self-gravity effect as well as the computational issue caused by the mutual gravitational forces can be found in reference [13].

### Keplerian Two-Body Model

The Keplerian orbital motion of an asteroid (prior to deflection and/or fragmentation) in a heliocentric elliptical orbit is simply described by

$$\ddot{\mathbf{r}} + \frac{\mu}{r^3} \mathbf{r} = 0 \quad (1)$$

where  $\mathbf{r} = X_c \mathbf{I} + Y_c \mathbf{J} + Z_c \mathbf{K}$  is the position vector of the asteroid center-of-mass from the center of the Sun,  $r = \sqrt{X_c^2 + Y_c^2 + Z_c^2}$ ,  $\mu \approx \mu_\odot = 132,715 \times 10^6 \text{ km}^3/\text{s}^2$ , and  $\{\mathbf{I}, \mathbf{J}, \mathbf{K}\}$  is a set of basis vectors for the Heliocentric-Ecliptic reference frame. A heliocentric elliptical orbit is illustrated in Fig. 1. In principle, equation (1) can be numerically integrated for given initial conditions  $\mathbf{r}(t_0)$  and  $\dot{\mathbf{r}}(t_0)$  to find its solution  $\mathbf{r}(t)$ . However, the Keplerian orbital motion is uniquely determined by the six classical orbital elements

$$(a, e, i, \Omega, \omega, t_p)$$

where  $a$  is the semimajor axis,  $e$  is the eccentricity,  $i$  is the orbit inclination angle,  $\Omega$  is the longitude of the ascending node,  $\omega$  is the argument of the perihelion,

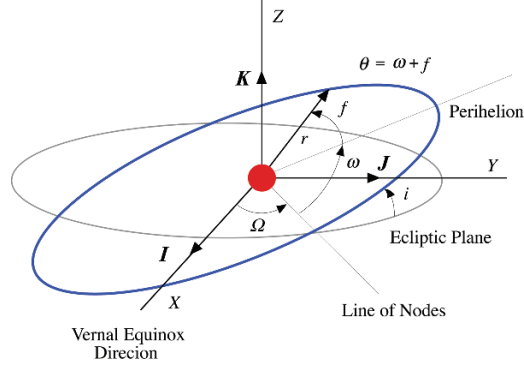


FIG. 1. Illustration of an Elliptical Reference Orbit of a Target NEO.

and  $t_p$  is the perihelion passage time (often replaced by the mean anomaly  $M_0$  at epoch).

It is assumed that a subsurface nuclear explosion results in instantaneous fragmentation of an asteroid, as illustrated in Fig. 2. The Keplerian orbital motion of each fragment is then described by

$$\ddot{\mathbf{R}} + \frac{\mu}{R^3} \mathbf{R} = 0 \quad (2)$$

where  $\mathbf{R} = X\mathbf{I} + Y\mathbf{J} + Z\mathbf{K}$  is the inertial position vector of a fragment and  $R = |\mathbf{R}| = \sqrt{X^2 + Y^2 + Z^2}$ . The relative position vector of a fragment from the center of mass,  $c$ , becomes

$$\delta \mathbf{r} = \mathbf{R} - \mathbf{r} = (X - X_c)\mathbf{I} + (Y - Y_c)\mathbf{J} + (Z - Z_c)\mathbf{K} \quad (3)$$

A rotating local-vertical and local-horizontal (LVLH) reference frame ( $x, y, z$ ) is employed to express the relative position vector of a fragment as

$$\delta \mathbf{r} = x\mathbf{i} + y\mathbf{j} + z\mathbf{k} \quad (4)$$

where ( $x, y, z$ ) are the radial, transverse, and normal components of the relative position vector in the LVLH frame. The origin of the LVLH frame is located at the

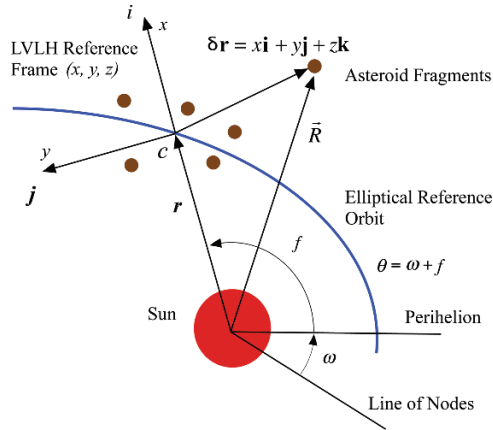


FIG. 2. Illustration of the Local-Vertical and Local-Horizontal (LVLH) Reference Frame.

center of mass of the unfragmented asteroid. Consequently, relationships between  $(x, y, z, \dot{x}, \dot{y}, \dot{z})$  and  $(X, Y, Z, \dot{X}, \dot{Y}, \dot{Z})$  can be defined as

$$\begin{bmatrix} x \\ y \\ z \end{bmatrix} = C \begin{bmatrix} X - X_c \\ Y - Y_c \\ Z - Z_c \end{bmatrix} \quad (5)$$

$$\begin{bmatrix} \dot{x} \\ \dot{y} \\ \dot{z} \end{bmatrix} = C \begin{bmatrix} \dot{X} - \dot{X}_c \\ \dot{Y} - \dot{Y}_c \\ \dot{Z} - \dot{Z}_c \end{bmatrix} - \begin{bmatrix} 0 & -\dot{\theta} & 0 \\ \dot{\theta} & 0 & 0 \\ 0 & 0 & 0 \end{bmatrix} \begin{bmatrix} x \\ y \\ z \end{bmatrix} \quad (6)$$

$$C = C_3(\theta)C_1(i)C_3(\Omega) = \begin{bmatrix} \cos\theta & \sin\theta & 0 \\ -\sin\theta & \cos\theta & 0 \\ 0 & 0 & 1 \end{bmatrix} \begin{bmatrix} 1 & 0 & 0 \\ 0 & \cos i & \sin i \\ 0 & -\sin i & \cos i \end{bmatrix} \cdot \begin{bmatrix} \cos\Omega & \sin\Omega & 0 \\ -\sin\Omega & \cos\Omega & 0 \\ 0 & 0 & 1 \end{bmatrix} \quad (7)$$

where  $(\theta, i, \Omega)$  are three angles associated with the nominal reference orbit,  $\theta = \omega + f$  is the true latitude, and  $f$  is the true anomaly.

#### *Solution to Kepler's Problem*

Given the initial relative position and velocity components of each fragment,  $(x, y, z, \dot{x}, \dot{y}, \dot{z})$ , the heliocentric position and velocity components,  $(X, Y, Z, \dot{X}, \dot{Y}, \dot{Z})$ , are determined as

$$\begin{bmatrix} X \\ Y \\ Z \end{bmatrix} = \begin{bmatrix} X_c \\ Y_c \\ Z_c \end{bmatrix} + C^T \begin{bmatrix} x \\ y \\ z \end{bmatrix} \quad (8)$$

$$\begin{bmatrix} \dot{X} \\ \dot{Y} \\ \dot{Z} \end{bmatrix} = \begin{bmatrix} \dot{X}_c \\ \dot{Y}_c \\ \dot{Z}_c \end{bmatrix} + C^T \left\{ \begin{bmatrix} \dot{x} \\ \dot{y} \\ \dot{z} \end{bmatrix} + \begin{bmatrix} 0 & -\dot{\theta} & 0 \\ \dot{\theta} & 0 & 0 \\ 0 & 0 & 0 \end{bmatrix} \begin{bmatrix} x \\ y \\ z \end{bmatrix} \right\} \quad (9)$$

Then, given the initial position and velocity vectors of a fragment (i.e.,  $\mathbf{R}_0$  and  $\mathbf{V}_0$  at  $t = t_0$ ), we can determine  $\mathbf{R}(t)$  and  $\mathbf{V}(t)$  by solving Kepler's problem as [14]

$$\begin{bmatrix} \mathbf{R}(t) \\ \mathbf{V}(t) \end{bmatrix} = \begin{bmatrix} F & G \\ \dot{F} & \dot{G} \end{bmatrix} \begin{bmatrix} \mathbf{R}_0 \\ \mathbf{V}_0 \end{bmatrix} \quad (10)$$

where  $F$  and  $G$  are the Lagrangian coefficients expressed as [14]

$$F = 1 - \frac{a}{R_0} (1 - \cos \Delta E) \quad (11a)$$

$$G = (t - t_0) - \sqrt{\frac{a^3}{\mu}} (\Delta E - \sin \Delta E) \quad (11b)$$

$$\dot{F} = -\frac{\sqrt{\mu a}}{RR_0} \sin \Delta E \quad (11c)$$

$$\dot{G} = 1 - \frac{a}{R} (1 - \cos \Delta E) \quad (11d)$$

$$R_0 = |\mathbf{R}_0|; R = |\mathbf{R}(t)|; \Delta E = E - E_0 \quad (11e)$$

and the semimajor axis  $a$  and  $\Delta E$  can be determined from the set of equations

$$\frac{V_0^2}{2} - \frac{\mu}{R_0} = -\frac{\mu}{2a} \quad (12)$$

$$R_0 = a(1 - e \cos E_0) \quad (13)$$

$$t - t_0 = \sqrt{\frac{a^3}{\mu}} [2k\pi + (E - e \sin E) - (E_0 - e \sin E_0)] \quad (14)$$

where  $k$  is the number of times the object passes through perihelion between  $t_0$  and  $t$ .

Equation (10) can also be written as [16]

$$[X \ Y \ Z \ \dot{X} \ \dot{Y} \ \dot{Z}]^T = \begin{bmatrix} F & I & G & I \\ \dot{F} & I & \dot{G} & I \end{bmatrix} [X_0 \ Y_0 \ Z_0 \ \dot{X}_0 \ \dot{Y}_0 \ \dot{Z}_0]^T \quad (15)$$

where  $I$  is a  $3 \times 3$  identity matrix. The  $6 \times 6$  matrix in equation (15) is not a state transition matrix because the Lagrangian coefficients ( $F$ ,  $G$ ) are also functions of the initial state vector  $(X_0, Y_0, Z_0, \dot{X}_0, \dot{Y}_0, \dot{Z}_0)$ .

### *Elliptical CWH Equations of Relative Motion*

The relative orbital motion of a fragment with respect to the LVLH reference frame of an elliptical reference orbit can also be directly described as [16]

$$\ddot{x} = \left( \frac{2\mu}{r^3} + \dot{\theta}^2 \right) x + 2\dot{\theta}\dot{y} + \ddot{\theta}y \quad (16a)$$

$$\ddot{y} = \left( -\frac{\mu}{r^3} + \dot{\theta}^2 \right) y - 2\dot{\theta}\dot{x} - \ddot{\theta}x \quad (16b)$$

$$\ddot{z} = -\frac{\mu}{r^3} z \quad (16c)$$

where  $\theta = f + \omega$  is the true latitude,  $f$  is the true anomaly, and  $\mu$  is the gravitational parameter of the Sun. It is assumed that  $\sqrt{x^2 + y^2 + z^2} < r$ . Equations (16) are called the elliptical Clohessy-Wiltshire-Hill (CWH) equations of motion in this paper.

The elliptical reference orbit is described by

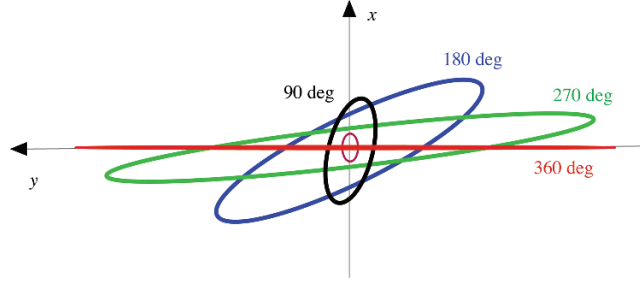


**FIG. 3.** Evolution of the Fragment Clouds in a Circular Orbit, with Increasing True Anomaly (for an Isotropic Distribution of Initial Dispersal Velocity).

$$\ddot{r} = r\dot{\theta}^2 - \frac{\mu}{r^2} \quad (17)$$

$$\ddot{\theta} = -\frac{2\dot{r}\dot{\theta}}{r} \quad (18)$$

Furthermore,

$$r = \frac{p}{1 + e \cos f} = \frac{p}{1 + e (\cos \omega \cos \theta + \sin \omega \sin \theta)} \quad (19a)$$

$$\dot{r} = \sqrt{\mu/p} (e \sin f) = \sqrt{\mu/p} e (\sin \theta \cos \omega - \cos \theta \sin \omega) \quad (19b)$$

$$\dot{\theta} = \sqrt{\mu/p^3} (1 + e \cos f)^2 = \sqrt{\mu/p^3} [1 + e (\cos \omega \cos \theta + \sin \omega \sin \theta)]^2 \quad (19c)$$

where  $p = a(1 - e^2)$ .

The elliptical CWH equations can be numerically integrated for orbital dispersion simulation and analysis of fragmented bodies. However, a state transition matrix (STM) approach can also be employed to avoid such direct numerical simulation of many fragments. This STM approach has been demonstrated in reference [18] to be computationally effective and accurate.

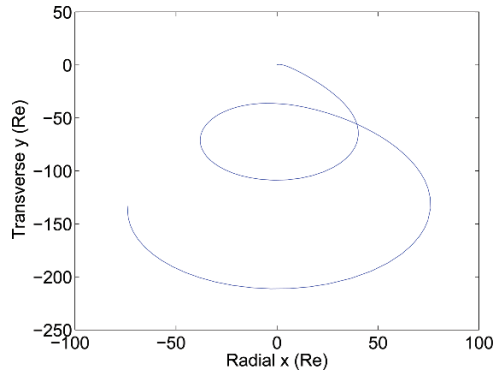


**FIG. 4.** Relative Motion of a Fragment in the LVLH Frame of a Reference Elliptical Orbit for Two Orbital Periods in Earth Radii (Re).

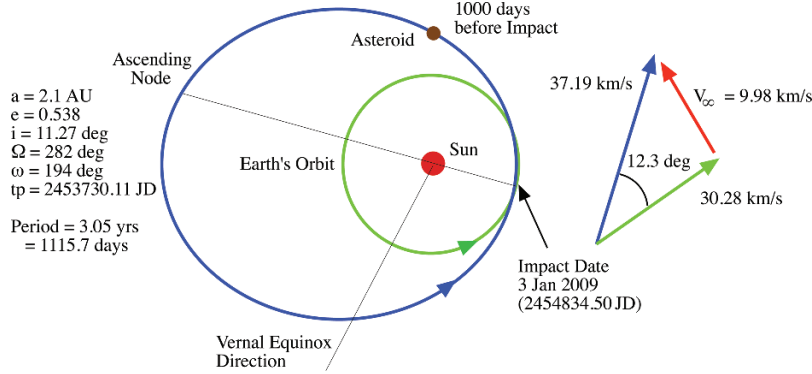


FIG. 5. A Fictive NEO in an Elliptical Orbit with Its Impact Date Of January 3, 2009.

### Relative Motion of Fragments in the LVLH Frame

Figure 3 shows the pattern of a debris cloud (in an ideal circular orbit) as a function of true anomaly for an isotropic distribution of initial relative velocity. After the first orbit, the debris cloud will look like a simple stretching along the orbital path. It should be mentioned that the characteristics of the orbit are the governing factors behind this phenomenon, and that all initial distributions with material at a nonzero distance from the center of mass will result in similar cloud shapes. A typical relative motion of a fragment, in the LVLH frame of an elliptical orbit with  $e = 0.538$ , with an initial dispersion velocity of 1 m/s along the orbital direction is shown in Fig. 4.

### Reference Elliptical Orbit and Hyperbolic Approach Orbit

In this paper, we consider a reference elliptical orbit of a fictive NEO as illustrated in Fig. 5. Its six classical orbital elements are provided in the figure. The impact parameter  $b$  of this fictive NEO, illustrated in Fig. 6, can be estimated as [14]

$$b = R_{\oplus} \sqrt{1 + \left(\frac{V_e}{V_{\infty}}\right)^2} \approx 1.5R_{\oplus} \quad (20)$$

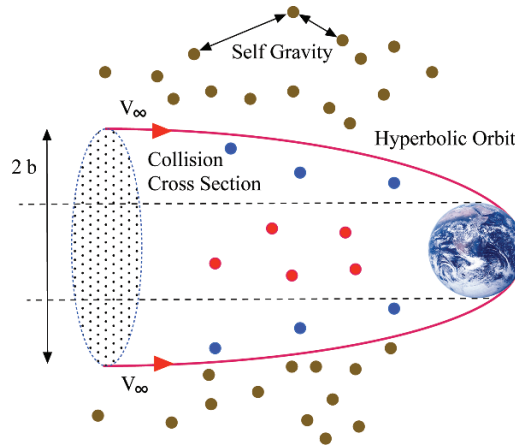


FIG. 6. Illustration of the Impact Parameter and the Collision Cross Section.



where  $V_e$  is the Earth escape speed of 11.2 km/s and  $V_\infty$  is the hyperbolic approach speed of this NEO ( $\approx 9.98$  km/s). This impact parameter determines the collision cross section, which can be used to analyze the fragmented system for bodies needing more precise calculations to determine the threat of impact.

## Nuclear Subsurface Explosion Models

### Gravitational Binding Energy

In astrophysics, the energy required to disassemble a celestial body consisting of loose material, which is held together by gravity alone, into space debris such as dust and gas is called the gravitational binding energy.

The gravitational binding energy of a spherical body of mass  $M$ , uniform density  $\rho$ , and radius  $R$  is given by [6]

$$E = \frac{3GM^2}{5R} = \frac{3G}{5R} \left( \frac{4\pi\rho R^3}{3} \right)^2 = \frac{\pi^2 \rho^2 G}{30} D^5 \quad (21)$$

where  $G = 6.67259 \times 10^{-11} \text{ N}\cdot\text{m}^2/\text{kg}^2$  is the universal gravitational constant and  $D = 2R$  is the diameter of a spherical body. The escape speed from its surface is given by

$$V_s = \sqrt{\frac{2GM}{R}} \quad (22)$$

For example, for a 200-m (diameter) asteroid with a uniform density of  $\rho = 2720 \text{ kg/m}^3$  and a mass of  $M = 1.1 \times 10^{10} \text{ kg}$ , its gravitational binding energy is estimated to be  $4.8 \times 10^7 \text{ J}$  and the escape speed from its surface is 12 cm/s. The escape speed from a 1-km asteroid is less than 1 m/s.

In references 1 and 2, the disruption energy per unit asteroid mass is predicted to be 150 J/kg for strength-dominated asteroids. Also in reference [2], the energy (per unit asteroid mass) required for both disruption and dispersion of a 1-km asteroid is predicted to be 5000 J/kg.

A 300 kt nuclear subsurface explosion has a sufficient energy of  $12 \times 10^{14} \text{ J}$  to disrupt and disperse a 200-m asteroid. A 1 Mt nuclear subsurface explosion has sufficient energy of  $4.18 \times 10^{15} \text{ J}$  to also disrupt and disperse a 1-km asteroid.

### Fragmentation Models

Nuclear energy densities are nearly a million times higher than those possible with chemical bonds, and thus it is the most mass efficient means for storing energy. For example, on the Earth's surface (in dry soil), a 1 Mt nuclear explosive device creates a crater that is about 150 m in radius and 75 m deep, ejecting approximately  $3.5 \times 10^9 \text{ kg}$  of material [13]. As discussed in reference [3], a nuclear excavation experiment showed that burial improves the energy coupling compared to an explosion on the surface and results in a much larger crater from a smaller yield device. This paper considers such a nuclear subsurface explosion with shallow burial for large diameter (1 km) as well as small diameter (270 m) models of NEOs.

Figure 7 illustrates a two-component (inhomogeneous) spherical structure with a high density core consistent with granite (density =  $2.63 \text{ g/cm}^3$ ), and a lower density ( $1.91 \text{ g/cm}^3$ ) mantle. The bulk density of the structure was  $1.99 \text{ g/cm}^3$ , close to that measured for asteroid Itokawa (density =  $1.95 \text{ g/cm}^3$ ) [19].

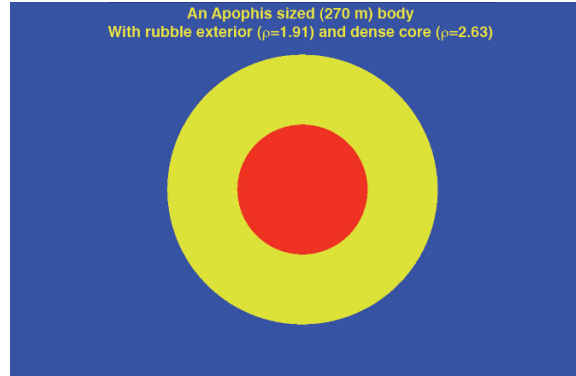


FIG. 7. Internal Composition Model of an Apophis-Sized (270 m) NEO.

A 1-km NEO model has a total mass of  $1.05 \times 10^{12}$  kg, or just over a billion tons, placing it in the class of potentially catastrophic impactors. The smaller, 270-m model was sized to approximate Apophis with a total mass of  $2.058 \times 10^{10}$  kg, or a bit over 20 million tons.

Sourcing energies corresponding to 900 kt into the 1-km model and 300 kt into the 270-m body simulated surface explosions. The source region is cylindrical, and the dimensions in the smaller body are 1 m in diameter and 5 m long, as illustrated in Fig. 8. This source volume is  $4.5 \text{ m}^3$  containing a bit over 8 tons of material. In the larger body, the source region has a volume near  $10 \text{ m}^3$ .

As shown in Fig. 9, two-dimensional hydrodynamic modeling of the subsequent explosion led to expanding clouds of debris. The structures were modeled with different strength approximations, including no material strength, a linear strength model (strength proportional to pressure, limited by a crush strength) often used for

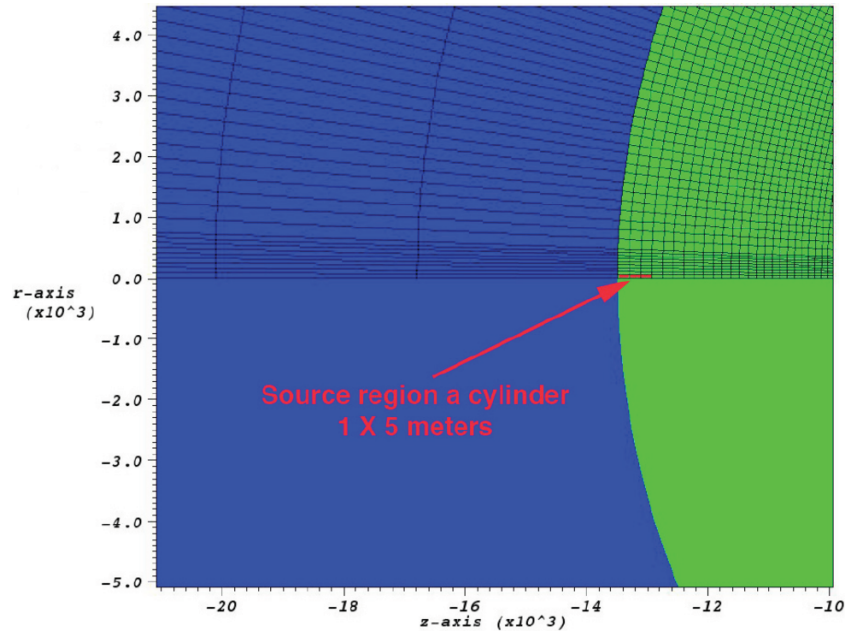


FIG. 8. Computational Modeling Illustration of Nuclear Subsurface Explosion.

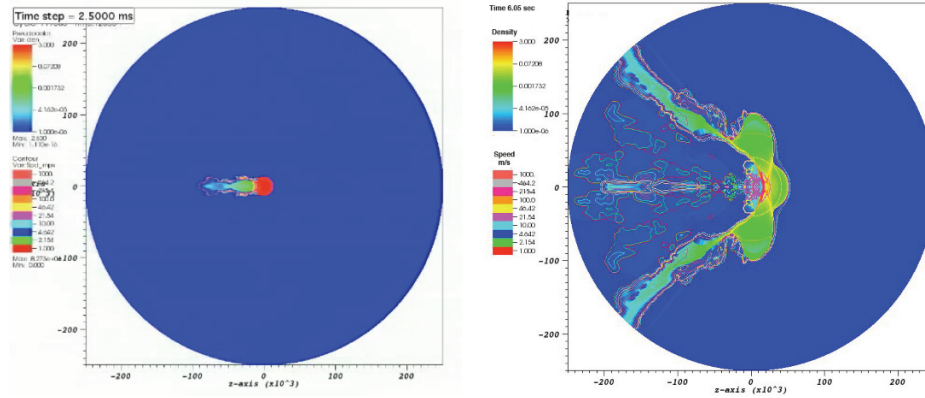


FIG. 9. Computational Results from the Hydrodynamic Code.

shock propagation in rubble, and a model that includes full strength in the core. The yield strength in the core is set to 14.6 MPa, with a shear modulus of 35 MPa. This is somewhat weaker than measured for most granite, and is near the low-end for limestone. These types of rocks have comparable density to that of the present model.

The energy source region expands, creating a shock that propagates through the body, resulting in fragmentation and dispersal. While the material representations used have been tested in a terrestrial environment, there are low-density objects, like Mathilde, where crater evidence suggests a very porous regolith with efficient shock dissipation. High bulk porosity may also be present in many Solar System bodies. Shock propagation may be less efficient in such porous material, generally reducing the net impulse from a given amount of energy coupled into the surface. More work is needed to understand the limits of very high porosity.

The models were evolved until the bodies had substantially expanded, and the velocity gradients indicated homologous expansion. After about 20 s, the large models showed material with expansion speeds up to 50 m/s. The mass averaged speed in the no-strength model (M97) was 12 m/s, and it was nearly 14 m/s in the linear-strength model (M20e). The smaller model (Ap300) was run with a linear-strength model, and after 6 s, the mass averaged speed of the fragments was near 50 m/s with peak near 30 m/s (Fig. 10).

A three-dimensional fragmentation model (Fig. 11) was then constructed from the 2D hydrodynamics models by interpolating the position, speed and mass of each zone, and rotating it to a randomly assigned azimuth about the axis of symmetry. For a 1-km NEO, two basic models (M97 and M20e) were developed. Both models sourced 900 kt into a surface region of the same 1 km diameter object, with an initial mass of  $1.047 \times 10^9$  tons. The difference in the two systems is that M97 was a finely zoned model compared to M20e. Approximately 20 s after the energy deposition, M97 had 31,984 zones of asteroid material for  $9.6732 \times 10^8$  tons, 92.8% of the initial mass. The missing 7.2% was ejected from the mesh at high speed prior to the end of the hydrodynamics simulation. In Fig. 12, the fragmentation model M97 for a 1-km NEO disrupted by 900 kt nuclear subsurface explosion is shown.

For intercept-to-impact times longer than 300 days, the models are interpolated dividing each 2D zone into 16 (M97) or 49 (M20e) fragments of equal masses. The

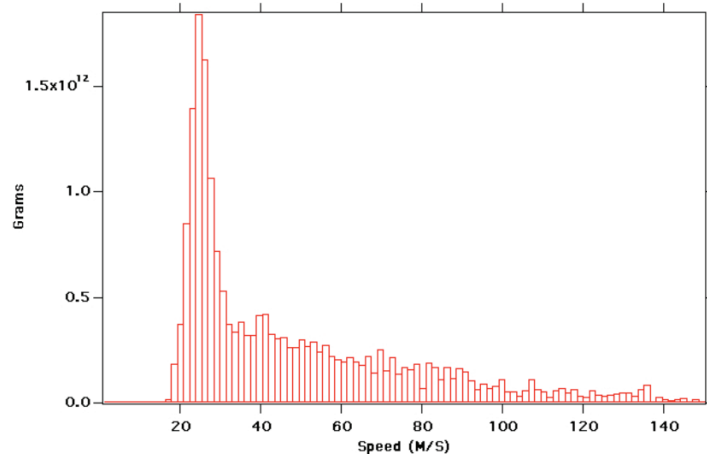


FIG. 10. Speed Distribution of the Fragmentation Model Ap300 (6 s After the Burst.)

position and velocity of these fragments are found by linearly interpolating from the position and speed of the four nodes defining the corners of the zone. The resulting M97i model, shown in Fig. 13, has 511,744 fragments while the M20e model has 105,742 fragments.

These 3D fragment distributions could then be placed and oriented on the asteroid trajectory at different times before impact. For example, the X-axis in Fig. 14 can be aligned with the orbital flight direction or some other direction. Sensitivity to the choice of this direction has been further addressed in reference [20].

## Results and Discussions

A computer code developed by the third author was used for orbital dispersion simulation and analysis. These results have been validated by the other authors using the various fundamental approaches of Keplerian orbital dynamics discussed in this paper, as well as the STM approach by the authors of reference [18]. References [20–22] continue this analysis to include the effects of self-gravity and sensitivity to lead-time and the initial energy.

To assess the degree of mitigation, the code includes gravitational focusing effect of the Earth on those fragments that pass near the Earth, and provide a census

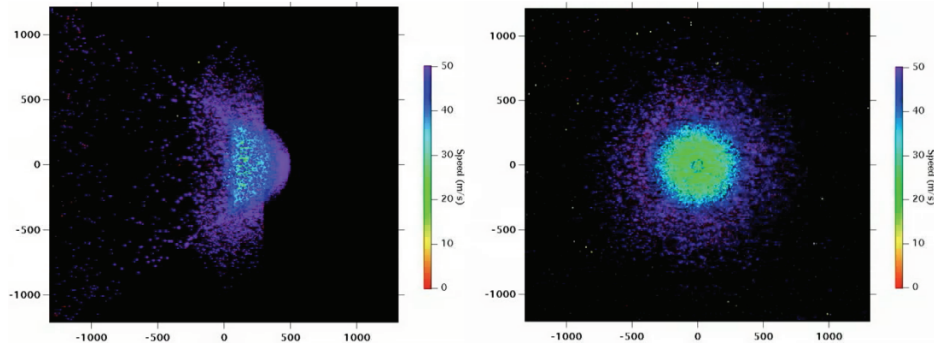


FIG. 11. Fragmentation Model Ap300, with 18,220 Fragments, for a 270-m NEO Disrupted by 300-kt Nuclear Subsurface Explosion.

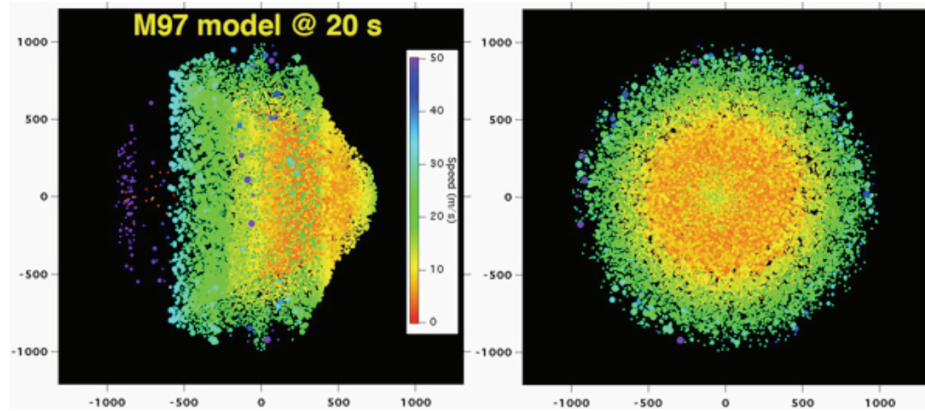


FIG. 12. Fragmentation Model M97, with 31,984 Fragments, for a 1-km NEO Disrupted by 900-kt Nuclear Subsurface Explosion.

of those that hit (with a minimum distance  $< 1$  Earth radius). The code then has two modes of use as described below.

(i) Orbital elements are evaluated for each fragment and the code is used to project the fragment forward in time. This is used to show the debris cloud evolution over the whole time from intercept to impact time.

(ii) The orbital elements of each fragment are used to define its position and velocity at a time just prior to the original impact date. Times ranging from five days to six hours prior to the nominal impact time can be selected. After the analytic step places the debris field near the Earth, the relative velocity of each fragment with respect to the Earth is used to calculate its closest approach. A subset of the fragments that will pass within 15 Earth radii is selected to reduce integration cost. These fragments are directly integrated, accounting for the gravity of the Earth and Moon.

Those fragments that pass within one Earth radius are impacts.

This selection process was tested up to five days out from nominal impact, and successfully identified the fragments that would pass nearer the Earth than the selected limit. Further, and as expected, changing the radius of the selected

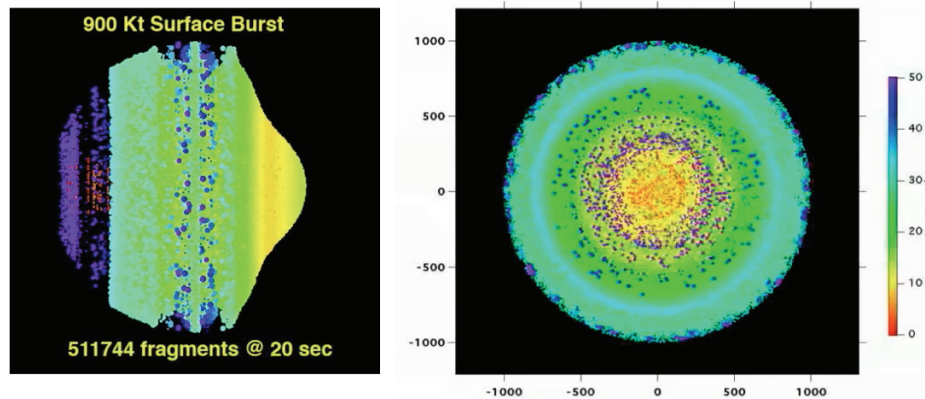
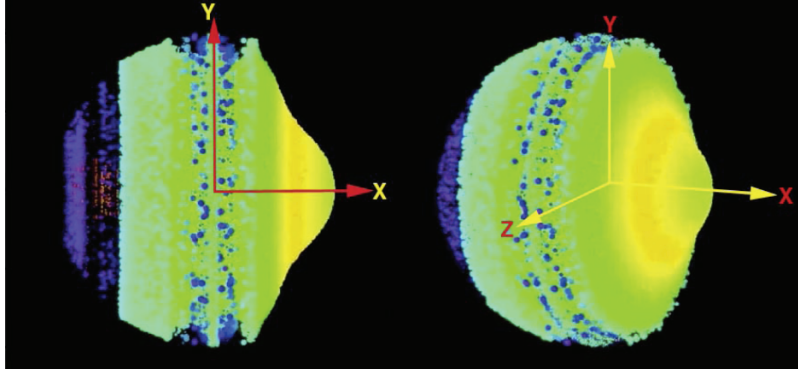


FIG. 13. Fragmentation Model M97i (interpolated), with 511,744 Fragments, for a 1-km NEO Disrupted by 900-kt Nuclear Subsurface Explosion.



**FIG. 14.** Coordinates for Initial Dispersion Position and Velocity Components.

cylinder from 15 to 5 Earth radii resulted in no change in the number of hits. While the direction of fragments that pass within a couple of Earth radii are strongly changed, the fragments near the outer portion of the selected group show only modest angular deviations. The two basic models M97 and M20e were tested first. Less material is lost from this simulation because the surrounding area was larger, and the run time was shorter. For 10 to 300 days to impact, these basic models with each zone treated as a fragment were usually sufficient to obtain enough hits to estimate the amount of mass that remained a threat. As the time to impact increases, the fragments become more dispersed, and number that hit decreases. When fewer than 10 fragments hit the Earth, the statistical measure of how much of the asteroid remains a threat is poor. When only a few fragments hit the Earth, the fraction of the asteroid mass that threatens (impacts) is merely suggestive of the actual impact probability.

Figure 15 summarizes the result of intercepting and disrupting a 1-km NEO with 900 kt nuclear subsurface explosion 1000 days before the impact date of January 3, 2009. For this case, the X-axis of the hydrodynamics fragmentation model has been aligned with the orbital flight direction and there are only 10 impacts with a total mass of 3000 tons. For an interception 100 days before impact, the M97 model (1/16th fragments of the M97i model) provides

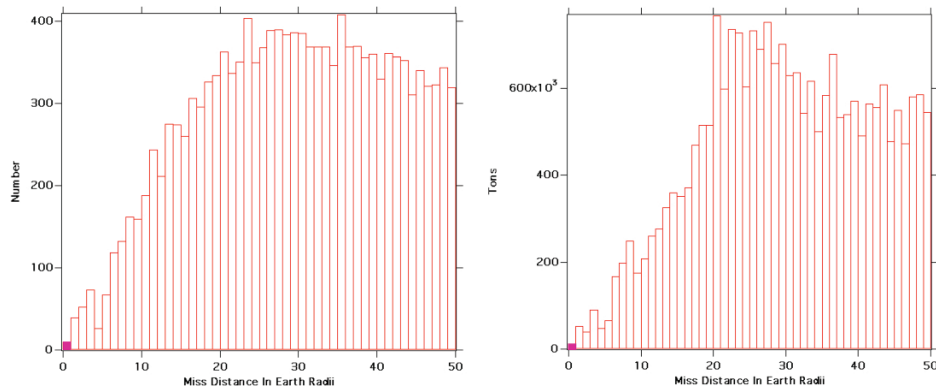


**FIG. 15.** Result of an Interception 1000 Days Before Impact for the Fragmentation Model M97i (1 km NEO).



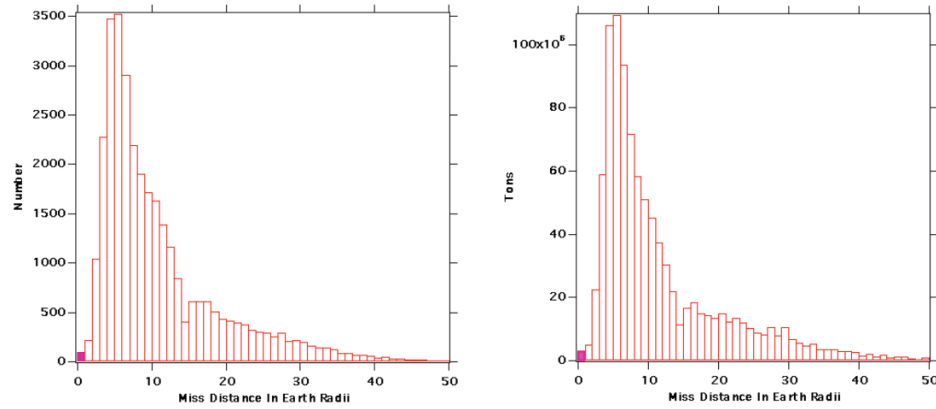


FIG. 16. Result of an Interception 100 days Before Impact for the Fragmentation Model M97 (1 km NEO).

sufficient impacts, and the histograms in Fig. 16 show more fragments pass near the Earth.

The result for the Ap300 model with 15 days before impact is provided in Fig. 17. Only 3% of the initial mass resulted in impacting the Earth even for such a very short time after interception. The impact mass can be further reduced to 0.2% if the X-axis of the hydrodynamic fragmentation model is aligned along the inward or outward direction of the orbit, i.e., perpendicular to NEO's orbital flight direction [20]. Such a sideways push is shown to be near-optimal when a target NEO is in the last orbit before the impact. However, a conservative estimation of the impact mass for a worst-case scenario is considered in this paper. The impact mass can be further reduced by increasing the intercept-to-impact time or by increasing the energy level of nuclear explosives (i.e., higher yields).

In Fig. 18, a performance summary of the nuclear subsurface explosions is presented. The mass that impacts the Earth is converted to energy using  $V_\infty$  of

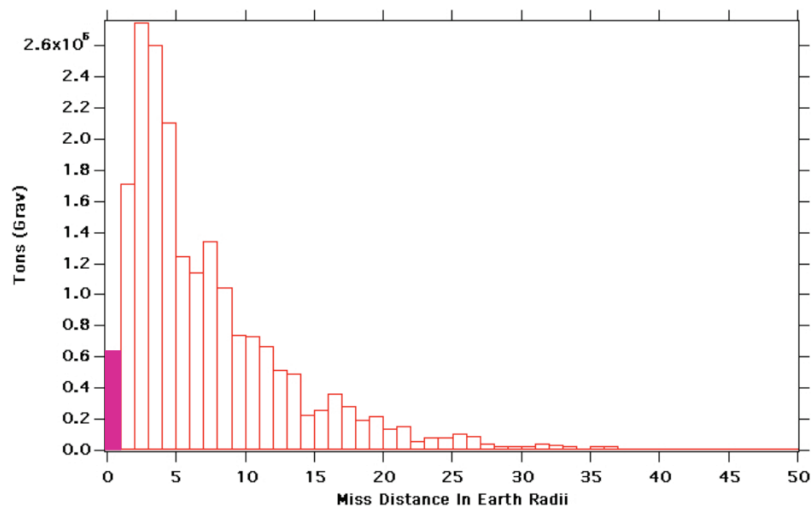


FIG. 17. Result of An Interception 15 days Before Impact for the Fragmentation Model Ap300 (270 m NEO).

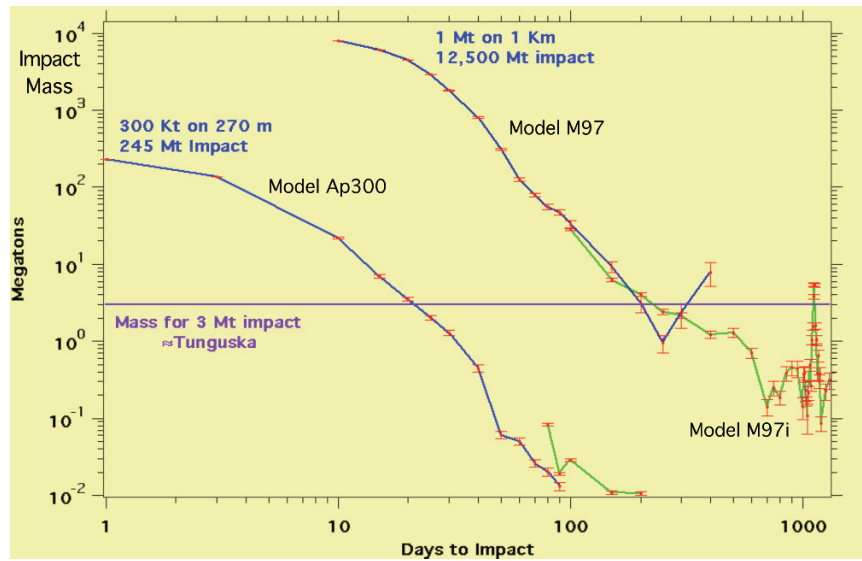


FIG. 18. Performance Summary of the Nuclear Subsurface Explosions (with Non-Optimal Interception and Shallow Burial of 5 m).

9.98 km/s. The simplest way of fragmenting the hydrodynamic model involves dividing it up based on the mesh. The results of this approach are shown in blue in Fig. 18. For longer periods the debris cloud is more dispersed, and there are not enough impacts to be statistically meaningful in determining the impact threat, due to the discrete set of fragments. For these longer flight times, more fragments were desirable and so the mesh of the hydrodynamic model was interpolated to create smaller (but more) fragments (results shown in green in Fig. 18).

From Fig. 18, a 1-Mt nuclear disruption mission for a 1-km NEO requires an intercept-to-impact time of 200 days to reduce the impact mass to that of the Tunguska event. Impacts of this energy are predicted to occur every 1000 years [23], and reduction to this energy would indicate protection from catastrophic ground impacts. A 270-m NEO requires an intercept-to-impact time of 20 days for its 300-kt nuclear disruption mission to reduce the impact mass to that of the Tunguska event. Therefore, it can be concluded that under certain conditions, disruption (with large dispersal) is a feasible strategy providing considerable impact threat mitigation for some representative worst-case scenarios. An optimal interception can further reduce the impact mass percentage shown in Fig. 18. However, a further study is necessary for assessing the effects of inherent physical modeling uncertainties and mission constraints.

### Future Research

For the most probable impact threat with a warning time much less than 10 years, the use of higher-energy nuclear explosives will become inevitable. Direct intercept missions with a short warning time will result in the arrival velocities of 2 to 30 km/s with respect to target asteroids. A rendezvous mission with target asteroids, requiring a large arrival  $\Delta V$  of 2 to 30 km/s, is impractical for many cases.



While a less destructive, standoff nuclear explosion can be employed for such direct intercept missions, the momentum/energy transfer created by a shallow subsurface nuclear explosion is roughly 100 times larger than that of a standoff nuclear explosion. However, the existing nuclear subsurface penetrator technology limits the impact velocity to less than 300 m/s because higher impact velocities prematurely destroy the detonation fusing devices. Also, a precision standoff explosion at an optimal height of burst near a irregularly shaped NEO, with intercept velocities as high as 30 km/s, is not a trivial task. Deviations from such an optimal height could result in a failed mission, or in disruption with low dispersion velocities.

Consequently, a hypervelocity nuclear interceptor system concept has been recently proposed and studied in references [24–26], which will enable a last minute, nuclear disruption mission with intercept velocities as high as 30 km/s. The proposed system employs a two-body space vehicle consisting of a fore body (leader) and an aft body (follower). The leader spacecraft provides proper kinetic impact crater conditions for the follower spacecraft carrying nuclear explosives to make a robust and effective explosion below the surface of a target asteroid body [24–26]. Surface contact burst or standoff explosion missions may not require such a two-body vehicle configuration, although they will require precision terminal guidance and control systems [27–28]. Furthermore, accurate and reliable prediction of Earth-impact probability of NEO fragments, including various orbital perturbation effects, will be required for real mission scenarios [29]. Robust nuclear deflection/disruption strategies and technologies, to be employed for a last minute direct intercept mission, need to be further studied, developed, and flight tested/validated.

## Conclusion

The orbital dispersion modeling, analysis, and simulation of a near-Earth object (NEO) fragmented and disrupted by nuclear subsurface explosions have been discussed in this paper. For some representative cases, this paper has shown that disruption using a nuclear subsurface explosion with shallow burial is a feasible strategy. However, more research work is needed to assess the effect of physical modeling uncertainties inherent to applying nuclear subsurface explosions to asteroid fragmentation and dispersion. The fundamental approaches of Keplerian orbital dynamics can still be effectively used for examining the orbital dispersion problem affected by various physical modeling uncertainties and space mission constraints (e.g., optimal approach angle, rendezvous versus intercept, impact penetration velocity, etc.).

## Acknowledgments

This research work by the first two authors was supported by a research grant from the Iowa Space Grant Consortium (ISGC) awarded to the Asteroid Deflection Research Center at Iowa State University. These authors would like to thank Dr. Ramanathan Sugumaran (Director, ISGC) for his support of this research work. Part of this work by the third author was performed under the auspices of the U.S. Department of Energy by Lawrence Livermore National Laboratory under Contract DE-AC52-07NA27344. The authors thank Dr. Daero Lee and Dakshesh Patel for validating the orbital dispersion analysis results of this paper by using the various fundamental approaches of Keplerian orbital dynamics, including the state transition matrix approach of reference [18].

## References

- [1] AHRENS, T. J. and HARRIS, A. W. "Deflection and Fragmentation of Near-Earth Asteroids," in *Hazards Due to Comets and Asteroids*, edited by GEHRELS, T., The University of Arizona Press, Tucson, AZ, 1994, pp. 897–927.
- [2] HOLSAPPLE K. A. "About Deflecting Asteroids and Comets," in *Mitigation of Hazardous Comets and Asteroids*, edited by BELTON, M. et al, Cambridge University Press, 2005, pp. 113–140.
- [3] DEARBORN, D. S. "21st Century Steam for Asteroid Mitigation," presented as paper AIAA-2004-1413 at the 2004 Planetary Defense Conference: Protecting Earth from Asteroids, Orange County, CA, Feb. 23–26, 2004.
- [4] ADAMS, R. B., ALEXANDER, R., BONOMETTI, J., CHAPMAN, J., FINCHER, S., HOPKINS, R., KALKSTEIN, M., POLSGROVE, T., STATHAM, G., and WHITE, S. *Survey of Technologies Relevant to Defense from Near-Earth Objects*, NASA-TP-2004-213089, NASA MSFC, July 2004.
- [5] DACHWALD, B. and WIE, B. "Solar Sail Kinetic Energy Impactor Trajectory Optimization for an Asteroid-Deflection Mission," *Journal of Spacecraft and Rockets*, Vol. 44, No. 4, 2007, pp. 755–764.
- [6] HANRAHAN, R. "Nuclear Explosives for NEO Deflection," Presented to Committee to Review Near-Earth Object Surveys and Hazard Mitigation Strategies: Mitigation Panel, National Research Council, March 30, 2009.
- [7] *Defending Planet Earth: Near-Earth Object Surveys and Hazard Mitigation Strategies*, Final Report, Committee to Review Near-Earth Object Surveys and Hazard Mitigation Strategies, National Research Council, The National Academies Press, January 2010.
- [8] WIE, B. "Dynamics and Control of Gravity Tractor Spacecraft for Asteroid Deflection," *Journal of Guidance, Control, and Dynamics*, Vol. 31, No. 5, 2008, pp. 1413–1423.
- [9] WAGNER, S., PITZ, A., ZIMMERMAN, D., and WIE, B. "Interplanetary Ballistic Missile (IPBM) System Architecture Design for Near-Earth Object Threat Mitigation," IAC-09-D1.1.1, 60th International Astronautical Congress, Daejeon, Korea, October 12–16, 2009.
- [10] WIE, B. "Astrodynamical Principles for Deflecting Hazardous Near-Earth Objects," John Breakwell Memorial Lecture, IAC-09-C1.3.1, 60th International Astronautical Congress, Daejeon, Korea, October 12–16, 2009.
- [11] SANCHEZ, J. P., VASILE, M., and RADICE, G. "On the Consequences of a Fragmentation due to a NEO Mitigation Strategy," 59th International Astronautical Congress, IAC-08-C1.3.10, Glasgow, U.K., 2008.
- [12] KAPLINGER, B. and WIE, B. "Orbital Dispersion Simulation of Near-Earth Objects Deflection/Fragmentation by Nuclear Explosions," IAC-09-C1.10.2, 60th International Astronautical Congress, Daejeon, Korea, October 12–16, 2009.
- [13] KAPLINGER, B., WIE, B., and DEARBORN, D. "Efficient Parallelization of Nonlinear Perturbation Algorithms for Orbit Prediction with Applications to Asteroid Deflection," presented as paper AAS 10–225 at the 20th AAS/AIAA Space Flight Mechanics Meeting, San Diego, CA, Feb. 15–17, 2010.
- [14] BATE, R., MUELLER, D., and WHITE, J. *Fundamentals of Astrodynamics*, Dover Publications, 1971, pp. 177–226.
- [15] WIE, B. *Space Vehicle Dynamics and Control*, AIAA Education Series, Second Edition, 2008, pp. 221–276.
- [16] SCHAUB, H. and JUNKINS, J. *Analytical Mechanics of Space Systems*, AIAA Education Series, 2003, pp. 593–674.
- [17] GIORGINI, J., BENNER, L., OSTRO, S., NOLAN, M., and BUSCH, M. "Predicting the Earth Encounter of 99942 Apophis," *Icarus*, Vol. 193, No. 1, 2008, pp. 1–19.
- [18] LEE, D., COCHRAN, J. E., and JO, J. H. "Solution to the Variational Equations for Relative Motion of Satellites," *Journal of Guidance, Control, and Dynamics*, Vol. 30, No. 3, 2007, pp. 669–678.
- [19] ABE, S., TADASHI, M., HIRATA, N., BARNOUIN-JHA, O. S., CHENG, A. F., DEMURA, H., GASKELL, R. W., HASHIMOTO, T., HIRAOKA, K., HONDA, T., KUBOTA, T., MATSUOKA, M., MIZUNO, T., NAKAMURA, R., SCHEERES, D. J., and YOSHIKAWA, M. "Mass and Local Topography Measurements of Itokawa," *Science*, 312, 2006, pp. 1344–1347.
- [20] KAPLINGER, B., WIE, B., and DEARBORN, D. "Preliminary Results for High-Fidelity Modeling and Simulation of Orbital Dispersion of Asteroids Disrupted by Nuclear Explo-

- sives,” presented as paper AIAA-2010-7982 at the AIAA/AAS Astrodynamics Specialist Conference, Toronto, Ontario, Canada, August 2–5, 2010.
- [21] KAPLINGER, B. and WIE, B. “Optimized GPU Simulation of a Disrupted Near-Earth Object Including Self Gravity,” presented as paper AAS-11-266 at the 21st AAS/AIAA Space Flight Mechanics Meeting, New Orleans, LA, February 13–17, 2011.
  - [22] KAPLINGER, B. and WIE, B. “Parameter Variation In Near-Earth Object Disruption Simulations Using GPU Acceleration,” presented as paper AAS-11-267 at the 21st AAS/AIAA Space Flight Mechanics Meeting, New Orleans, LA, February 13–17, 2011.
  - [23] HARRIS, A. “Update of Estimated NEO Population and Current Survey Completion,” *Proceedings of 2nd IAA Planetary Defense Conference*, Bucharest, Romania, May 9–12, 2011.
  - [24] WIE, B. “Hypervelocity Nuclear Interceptors for Asteroid Deflection or Disruption,” *Proceedings of 2nd IAA Planetary Defense Conference*, Bucharest, Romania, May 9–12, 2011.
  - [25] KAPLINGER, B. and WIE, B. “NEO Fragmentation and Dispersion Modeling and Simulation,” *Proceedings of 2nd IAA Planetary Defense Conference*, Bucharest, Romania, May 9–12, 2011.
  - [26] KAPLINGER, B. and WIE, B. “Comparison of Fragmentation/Dispersion Models for Asteroid Nuclear Disruption Mission Design,” presented as paper AAS 11-403 at the AAS/AIAA Astrodynamics Specialist Conference, Girdwood, AK, August 1–4, 2011.
  - [27] HAWKINS, M., GUO, Y., and WIE, B. “Guidance Algorithms for Asteroid Intercept Missions with Precision Targeting Requirements,” presented as paper AAS 11-531 at the AAS/AIAA Astrodynamics Specialist Conference, Girdwood, AK, August 1–4, 2011.
  - [28] GUO, Y., HAWKINS, M., and WIE, B. “Optimal Feedback Guidance Algorithms for Planetary Landing and Asteroid Proximity Operations,” presented as paper AAS 11-588 at the AAS/AIAA Astrodynamics Specialist Conference, Girdwood, AK, August 1–4, 2011.
  - [29] PITZ, A., TEUBERT, C., and WIE, B. “Earth-Impact Probability Computation of Disrupted Asteroid Fragments Using GMAT/STK/CODES,” presented as paper AAS 11-408 at the AAS/AIAA Astrodynamics Specialist Conference, Girdwood, AK, August 1–4, 2011.